MECHANISM OF KEYHOLE FORMATION AND STABILITY IN STATIONARY LASER WELDING

Jae Y. Lee[1*], Sung H. Ko[2] and Choong D. Yoo[1]

[1]Dept. of Mech. Eng., KAIST,
373-1 Kusong-dong, Yusong-gu, Daejon, Korea, mecca@kaist.ac.kr
[2]Research Engineer, Hyundai Heavy Industry,
1-1 Jounha-dong, Dong-gu,Ulsan, Korea, postdoc72@hanmail.net

Abstract

The formation and stability of stationary laser weld keyholes are investigated using a numerical simulation. The effect of multiple reflections in the keyhole is estimated using the ray tracing method, and the free surface profile, flow velocity and temperature distribution are calculated numerically. In the simulation, the keyhole is formed by the displacement of the melt induced by evaporation recoil pressure, while surface tension and hydrostatic pressure oppose cavity formation. At laser powers of 500W and greater, the protrusion occurs on the keyhole wall, which results in keyhole collapse and void formation at the bottom. Initiation of the protrusion is caused mainly by collision of upward and downward flows due to the pressure components.

Keywords

Laser welding, Keyhole formation and stability, Multiple reflections, Recoil pressure, Protrusion

1. Introduction

A distinctive feature of high power laser welding is keyhole formation. When the beam is focused to power densities on the order of 10^5 W/cm^2, strong evaporation occurs on the melt surface. Understanding and controlling keyhole variations is a problem of much practical importance because they affect the quality and consistency of the finished weld.

Major terms relating to the keyhole pressure balance are evaporation recoil pressure, hydrodynamic pressures (melt and plume), hydrostatic pressure and pressure due to surface tension[1]. In order to estimate these pressure components, it is necessary to calculate the free surface profile and temperature distribution of a keyhole. Modeling keyhole dynamics is thus basically a fluid dynamics problem with laser energy being the dominant factor in the energy equation. Laser energy that enters the keyhole is delivered to the wall directly by Fresnel reflection and indirectly by absorption and thermal transport in the keyhole plume. When the energy delivery by Fresnel reflection is of primary importance, multiple reflection of the laser beam enhances absorption along the keyhole depth, and affects local melting, evaporation and recoil pressure. As a result, the free surface profile, flow velocity and temperature distribution are coupled in a complex way.

Recent literature contains a number of reports of research pertaining to laser weld keyhole formation and dynamics. The equilibrium keyhole radius and its stability were predicted from steady-state solutions of pressure and energy balance equations [2]. The dynamic behavior was calculated from fluid dynamics perturbation analysis [3,4] and compared to experimental optical signal fluctuations [4]. Steady-state keyhole profiles were calculated from solutions of the energy balance equation with absorbed laser power due to multiple reflection estimated using the ray tracing method [5,6]. Keyhole profiles were calculated from solutions of energy and pressure balance equations with absorbed laser power estimated from simplified plume absorption and Fresnel reflection analyses. [7,8]. The level set method was employed recently to compute the keyhole formation dynamics such as the surface profile and flow velocity under various conditions [9].

It is obvious from the previous works that recoil pressure and multiple reflection are the important factors for keyhole formation. However, effects of molten metal flow and causes of keyhole instability have not been fully understood. In this work, dynamic behavior of the stationary keyhole is calculated numerically, and the mechanisms of keyhole formation and instability are investigated using the simulation results.

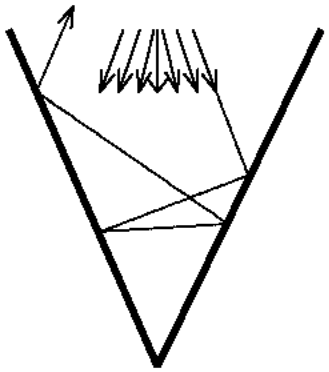

Fig.1 Schematic of multiple reflections on conical cavity

2. Modeling of Keyhole Dynamics

Multiple reflection within the keyhole, as illustrated in Fig.1 for a simple conical shape, increases absorption of the laser power by trapping the beam within the cavity. The ray tracing method is used in this work to estimate beam propagation. The incident laser beam is assumed to consist of rays, and the power of each ray is assigned from a circularly symmetric Gaussian beam profile. The ray tracing proceeds under the assumptions that the molten metal surfaces is specular, that plume absorption is negligible and that the beam polarization is random. Consistent with the last assumption, the reflectivity of the metal surfaces is taken as the intermediate value between available "s" and "p" reflectivity vs. angle curves. The number of reflections and the accumulated power density are calculated at each position on the keyhole wall, and the absorbed power density is estimated using Fresnel reflection as[5]:

$$\alpha_\theta = 1 - R_\theta = 1 - \frac{1}{2}\left(\frac{1+(1-\varepsilon\cos\theta)^2}{1+(1+\varepsilon\cos\theta)^2} + \frac{\varepsilon^2 - 2\varepsilon\cos\theta + 2\cos^2\theta}{\varepsilon^2 + 2\varepsilon\cos\theta + 2\cos^2\theta}\right) \qquad (1)$$

where θ represents the incident beam angle and ε is the function of dielectric constant, electric conductivity of matal and laser frequency. The absorbed power density is given as the boundary condition to calculate the temperature of the molten pool and workpiece.

The axi-symmetric keyhole profile and flow velocity are calculated numerically using the Volume of Fluid (VOF) method [10,11].

The temperature distribution is obtained by solving the energy equation as:

$$C_p\left(\frac{\partial T}{\partial t} + \bar{v} \cdot \nabla T\right) = k\nabla^2 T \qquad (2)$$

where C_p is the specific heat and k the thermal conductivity. The cooling effect of vapor leaving the surface is neglected in this energy equation. When the temperature on the free surface is obtained from the energy equation, the recoil pressure can be estimated. The recoil pressure due to evaporation is taken as 0.54 times the vapor pressure in equilibrium on the liquid surface, which is a common assumption implying that vapor flow velocity is at its maximum possible value [12]. The equilibrium vapor pressure is calculated from the integral of the Clausius-Clapeyron equation as:

$$P_r \cong 0.54 P_0 \exp\left(\Delta H_V \frac{T - T_V}{RTT_V}\right) \qquad (3)$$

where P_0 denotes atmospheric pressure, R the universal gas constant, ΔH_V the latent heat of vaporization and T_V the evaporation temperature. The recoil pressure is imposed on the free surface as the boundary condition.

Since the VOF method has been explained in detail in other reports [10,11], the calculation procedure is briefly summarized as follows: (1) absorbed laser power density on the keyhole wall is estimated using the ray tracing method, (2) temperature distribution is calculated by solving the energy equation, (3) recoil pressure is obtained from the surface temperature and imposed on the free surface, (4) free surface profile and liquid flow velocities are calculated numerically using the VOF method, (5) time is incremented and steps (1)-(5) are repeated.

3. Results and Discussions

In order to assess and illustrate the effect of multiple reflection on the power density distribution within a keyhole, ray tracing is performed for a conical cavity in Fig.1 having depth of 1mm and angle of 30°. The cavity is illuminated by 100W laser having Gaussian distribution, beam spot radius of 0.3mm and focal length of 100mm. In order to yield a smooth incident power density profile, ten rays are assigned to each VOF simulation grid cell having 0.02mm length, and the absorbed power density on the cavity walls is calculated using Fresnel reflection as shown in Fig.2. The absorbed power density increases rapidly at 0.6mm due to multiple reflections. Thus, much larger recoil pressure is exerted on the keyhole surface below 0.6mm because the heat is concentrated at the keyhole bottom.

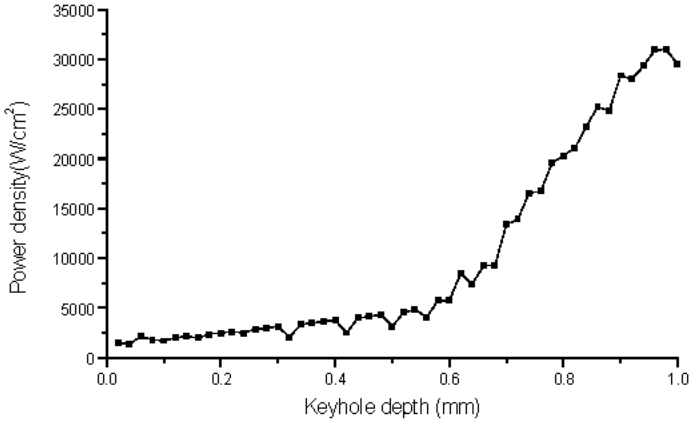

Fig.2 Absorbed power density on conical cavity using Fresnel reflection

Table 1 Material properties of mild steel and constants for calculation

mass density, ρ	7860 kg/m^3
kinematic viscosity, ν	5.6×10^{-7} m^2/s
surface tension coefficient, γ	1.2 N/m
thermal conductivity, κ	30 W/mK
specific heat , C_p	795 J/kgK
latent heat of vaporization, ΔH_v	6084 kJ/kg
Evaporating temperature, T_v	3130 K

Dynamic behaviors of the keyhole are simulated for the laser powers of 200W, 500W and 2kW using the same parameters as Fig.2. The material properties of the mild steel and constants listed in Table 1 are used for calculation. The keyhole profile and flow pattern corresponding to 200W laser power are shown in Fig.3. Surface depression of the molten pool is negligible because of the low laser power. As the calculated flow velocity is low, it has only limited effects on heat transfer and molten pool geometry. The melt shape corresponds to that of the conduction mode laser welding, which is similar to the melt geometries in arc welding [11].

When the laser power increases to 500W, the calculated surface profile, flow velocity distribution are illustrated in Figs.4. Simulation results show that the keyhole is formed and the molten metal oscillates upward and downward along the keyhole wall, a motion which appears to contribute to keyhole instability. Upward flow from the bottom of the keyhole, caused by recoil pressure at that location, delivers heat and molten metal to the upper portion of the keyhole. The upper portion becomes a convex profile, which produces the hydrostatic pressure and pressure due to surface tension. These pressures induce a downward flow opposite to the upward flow by recoil pressure. As the opposing flows collide at 8.6ms, an inward protrusion is formed near the keyhole entrance. Once the protrusion is

formed, it grows larger and eventually closes the cavity at 9.2ms. Several voids are trapped within the liquid at the keyhole bottom during this collapse. Although the keyhole is generated with 500W laser power, the molten metal layer on the keyhole wall is relatively thick so that the molten pool geometry is similar to that of the conduction mode. It is thus speculated that transition between the conduction and keyhole mode may occur near this power level.

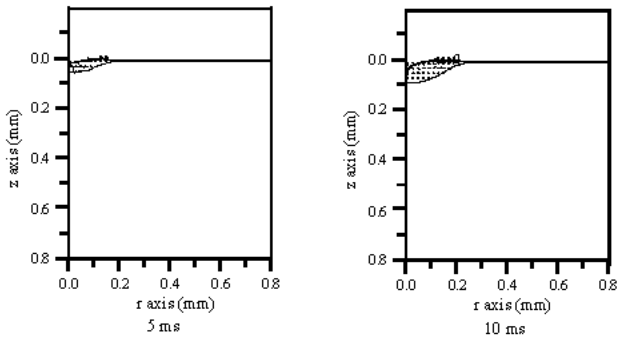

Fig.3 Surface profile and flow pattern for 200W laser

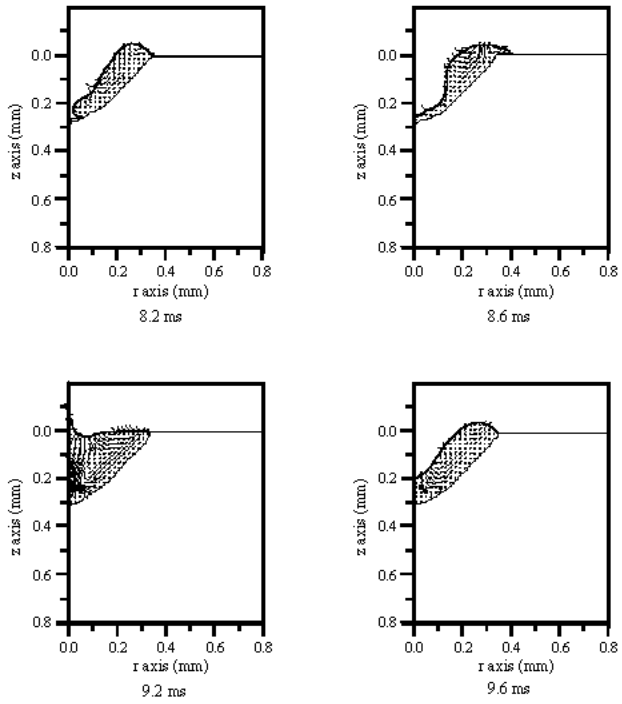

Fig.4 Surface profile and flow pattern for 500W laser

Fig.5 illustrate the keyhole profile and flow velocity distribution for 2kW laser. The keyhole forms rapidly at 5.35ms and the molten metal layer near the keyhole bottom becomes very thin due to high recoil pressure. Although the flow momentum from the keyhole bottom is large, the momentum appears to be dissipated by the viscous shear

stress generated at the thin molten layer on the keyhole wall (i.e., $\tau = -\mu \partial v/\partial z$). High flow velocity along the keyhole wall and thin molten metal layer thickness combine to produce large viscous shear stress, which dissipates the flow momentum. Since the decreased flow momentum is not sufficient to overcome the restraining pressure of surface tension, the molten metal layer becomes thicker near the cavity entrance and surface tension pressure subsequently causes a downward flow. A protrusion is visible on the keyhole wall at 5.4ms near z = 0.35mm. The protrusion slides down to the keyhole bottom due to recoil pressure at 5.45ms, and eventually closes the keyhole, leaving a void at the bottom at 5.5ms. The pool surface is then depressed to the void at the bottom at 5.55ms by recoil pressure, and the whole process repeats periodically in a similar fashion. It is noted that this collapse behavior by the protrusion has also been observed experimentally in high speed x-ray images of stationary laser weld keyholes [13], and similar phenomena were speculated in the cases of laser and electron beam welding [14, 15].

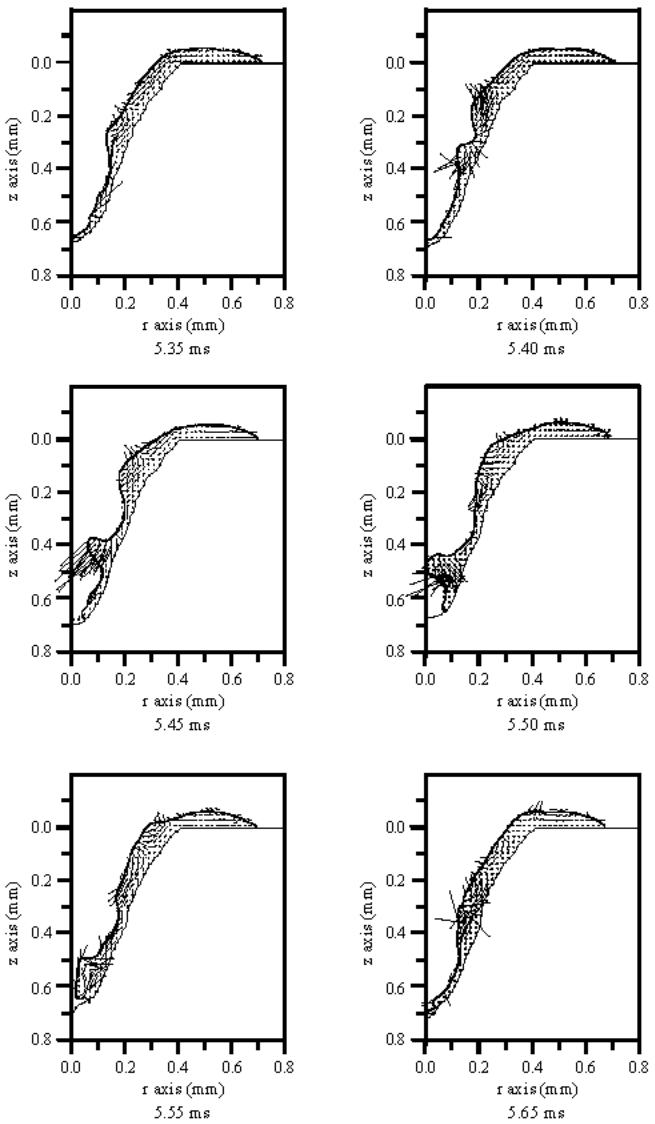

Fig.5 Surface profile and flow pattern for 2kW laser

Effects of the protrusion on calculated absorbed power densities at the keyhole surface for the 2kW simulation are shown in Fig.6. Since the protrusion absorbs the laser power and blocks the beam path, the distribution of the absorbed power density with protrusion becomes different from that of the normal keyhole in Fig.2. While the absorbed power at the protrusion is small at 5.4ms, it is much larger at 5.45ms due to the larger size of the protrusion. Therefore, occurrence of the protrusion appears to be the main cause of keyhole instability and void formation.

The simulation results provide some insight into keyhole dynamics and stability. In the initial stage of keyhole formation with small keyhole depth, the melt is easily forced up and out of the keyhole by recoil pressure. As keyhole depth increases, the viscous shear stress reduces the flow momentum, and the downward flow is generated at the keyhole entrance by hydrostatic pressure and surface tension. The protrusion is formed by collision of the opposing flows, which results in keyhole collapse and void formation. While the protrusion occurs at the entrance of the keyhole at 500W laser, it is formed near the middle of the keyhole depth at higher power of 2kW. Therefore, the keyhole becomes unstable even in the stationary condition, and considerations should be given on the effects of the viscous shear stress and protrusion formation on keyhole dynamics and stability.

It should be noted that the effects of pressure by hot gas mixture of the metal vapor and plasma within the cavity have not been considered in this work. This additional pressure and the gas flow within the cavity may influence the keyhole dynamics and stability. Further studies on the influence of the vapor and plasma within the cavity as well as the full penetration condition are needed.

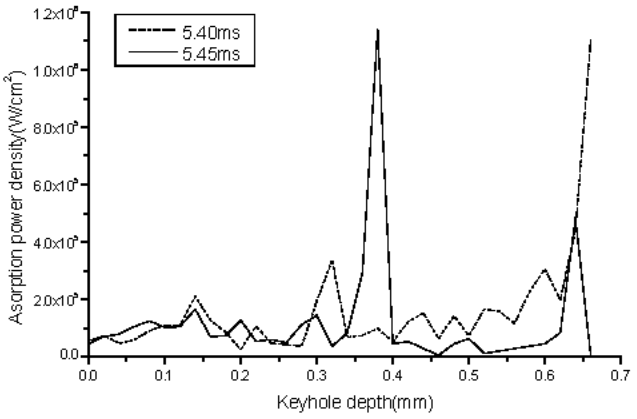

Fig.6 Variation of absorbed power densities for 2kW laser

4. Conclusions

Dynamic behavior of the keyhole is calculated numerically, and the mechanism of keyhole formation and stability in laser welding are analyzed based on the simulation results. The simulation results lead to the following conclusions.

(1) While high recoil pressure is exerted on the keyhole, especially at the bottom, it is not sufficient to eject the melt

entirely out of the cavity because the upward flow momentum from the keyhole bottom is reduced by the viscous shear stress on the keyhole wall.

(2) The keyhole is unstable even in the stationary condition due to its oscillating movement, and the protrusion is the main cause of keyhole collapse and void formation. The protrusion is initiated by collision of the upward and downward flows due to recoil pressure and surface tension, respectively.

(3) Transition between the conduction and keyhole modes exists at some laser power level, 500W in this work, which may be defined to have the pool geometry of the conduction mode with keyhole formation.

Acknowledgement

This work was supported by the BK-21 project and Kosef (No.996-1000-002-2).

References

[1] W. W. Duley :*Laser welding*, A Wiley Interscience Publication, (1999).

[2] J. Kroos , U. Gratzke and G. Simon : *J. Phys. D: Appl. Phys.*, 26(1993), p.474.

[3] J. Kroos, U. Gratzke, M. Vicanek and G. Simon : *J. Phys. D: Appl. Phys.*, 26(1993), p.481.

[4] T. Klein, M. Vicanek and G. Simon : *J. Phys. D: Appl. Phys.*, 29(1996), p.322.

[5] P. Solana and G. Negro : *J. Phys. D: Appl. Phys.*, 30(1997), p.3216.

[6] J. O. Milewski and M. B. Barbe : *Welding J.*,78(1999), p.109s.

[7] P. Solana and J. L. Ocaña : *J. Phys. D: Appl. Phys.*, 30(1997), p.1300.

[8] J. Dowden and P. Kapadia : *J. Phys. D: Appl. Phys.*, 28(1995), p.2252.

[9] H. Ki, P. S. Mohanty and J. Mazumder : *J. Phys. D: Appl. Phys.*, 34(2001), p.364.

[10] C. W. Hirt and B. D. Nichols : *J. of Computational Phys.*, 39(1981), p.201.

[11] S. H. Ko, S. K. Choi and C. D. Yoo : *Welding J.*, 80(2001), p.39s.

[12] M. von Allmen and A. Blatter : *Laser-beam interactions with materials*,Springer, (1995)

[13] M. Cho and D. Farson : *Proc. ICALEO'01*, (2001).

[14] M. Pastor, H. Zhao and T. Debroy : *Welding Int.*,15(2001), p.275.

[15] D. A. Schauer and W. H. Giedt : *Welding J.*, 57(1978), p.190s.